Microplankton Discrimination in FlowCAM Images Using Deep Learning*

Francisco Bonin-Font[1][a], Gorka Buenvaron[2], Mary K. Kane[3] and Idan Tuval[3]
[1]*Systems, Robotics and Vision Group (SRVG), University of the Balearic Islands, ctra de Valldemossa km 7.5, Palma de Mallorca, Balearic Islands, Spain*
[2]*Institute for Cross-Disciplinary Physics and Complex Systems (IFISC), University of the Balearic Islands, ctra de Valldemossa km 7.5, Palma de Mallorca, Balearic Islands, Spain*
[3]*Department of Marine Ecology, Mediterranean Institute of Advanced Studies (IMEDEA), Miquel Marqués 21, Esporles, Balearic Islands, Spain*

Keywords: Phytoplankton, Zooplankton, Convolutional Neural Networks.

Abstract: Marine plankton are omnipresent throughout the oceans, and the Mediterranean Sea is no exception. Innovation on microscopy technology for observing marine plankton over the last several decades has enabled scientist to obtain large quantities of images. While these new instruments permit generating and recording large amounts of visual information about plankton, they have produced a bottleneck and overwhelmed our abilities to provide meaningful taxonomic information quickly. The development of methods based on Artificial Intelligence or Deep Learning to process these images in efficient, cost-effective manners is an active area of continued research. In this study, Convolutional Neural Networks (CNNs) were trained to analyze images of natural assemblages of microplankton ($< 100\mu m$) and laboratory monocultures. The CNN configurations and training were focused on differentiating phytoplankton, zooplankton, and zooplankton consuming phytoplankton. Experiments reveal high performance in the discrimination of these different varieties of plankton, in terms of Accuracy, Precision, F1 scores and mean Average Precision.

1 INTRODUCTION

Marine phytoplankton are the base of most marine ecosystems. In the Mediterranean, algal blooms which cause harm to the environment, economy, and human health, also known as Harmful Algal Blooms (HABs), are increasing in frequency (Zingone et al., 2021). Along the Spanish and Balearic coast, HABs caused by dinoflagellates occur frequently in summer driven by pervasive sea breezes that push plankton towards the shore (Basterretxea et al., 2007) (Figueroa et al., 2008). Submarine groundwater discharges also provide increased nutrient concentrations nearshore, creating optimal conditions for phytoplankton growth (Tovar-Sánchez et al., 2014) (Rodellas et al., 2015). Being able to sample local blooms and identify potentially toxic species of dinoflagellates from other microplankton may enable us to create an early warning system and avoid harm to human health (Buskey and Hyatt, 2006) (Henrichs et al., 2021). Novel methods to classify and quantify plankton populations created in the last several decades have increased the speed and accuracy of their identification. Traditional microscopy involves looking at samples under a microscope and can be very time consuming, depending on the quantity of data and the ability of the involved technicians (Menden-Deuer et al., 2020). Flow cytometry permits a fast resolution of the size particles within a sample, but it does not always gives an accurate identification of plankton (Dubelaar and Jonker, 2000). Instruments like the FlowCAM and FlowCytobot generate images of plankton from water sam-

[a] https://orcid.org/0000-0003-1425-6907

*This work is partially supported by "ERDF A way of making Europe", Grant PLEC2021-007525/AEI/10.13039/501100011033 funded by the Agencia Estatal de Investigación, under Next Generation EU/PRTR, Grant PID2020-115332RB-C33 funded by MCIN/AEI/10.13039/501100011033, Grant JAEICU-2021-IMEDEA-07, funded by AEI, and by European Union's Horizon 2020 research and innovation programme funds under the Marie Skłodowska-Curie grant agreement No. 896043. The present research was carried out within the framework of the activities of the Spanish Government through the "Maria de Maetzu Center of Excellence" accreditation to IMEDEA (CSIC-UIB) (CEX2021-001198).

Bonin-Font, F., Buenvaron, G., Kane, M. and Tuval, I.
Microplankton Discrimination in FlowCAM Images Using Deep Learning.
DOI: 10.5220/0012460200003660

In *Proceedings of the 19th International Joint Conference on Computer Vision, Imaging and Computer Graphics Theory and Applications (VISIGRAPP 2024) - Volume 4: VISAPP*, pages 606-613
ISBN: 978-989-758-679-8; ISSN: 2184-4321

ples, creating a digital record which can be opened publicly to be used and referenced by multiple scientists (Ullah et al., 2022) (Yamazaki, 2022). However, having thousands of images of different plankton to obtain meaningful data is usually infeasible for a single person, creating a bottleneck. This problem is difficult to solve without using innovative automatic image classification algorithms based on Machine or Deep Learning.

Computers have become more powerful, and cloud-based servers or super-computers enable the processing of ever-larger quantities of data. Improvements in Artificial Intelligence (AI), Machine Learning and Neural Networks have produced impressive advances in visual object recognition, including automated detection and identification of plankton (Kerr et al., 2020) (Zhang et al., 2021) (Fuchs et al., 2022) (Zhang et al., 2023) (Sosa-Trejo et al., 2023). Although these advances have greatly enhanced our ability to classify organisms from images of natural populations, state of the art approaches and public image databases are not always applicable for localized studies and often need to be refined before use, leaving a wide range of possibilities for innovation. The work presented in this paper goes one step forward in using CNNs to detect and classify plankton compared to previous approaches with respect to the quality and origin of images used; the software platform used to implement, train, and validate the system; and the localized character of the problem to which the CNNs have been applied. Training, Validation and Testing datasets are partially formed from a time series of microplankton photography taken with a FlowCAM VS series (Yokogawa Fluid Imaging Technologies, Inc.) (Yokogawa, 2023) and collected at Cala Santanyí, Mallorca, (Spain). Unlike previous approaches, our work was centered on, in a first phase, discriminating autotrophic from heterotrophic microplankton, including heterotrophic microplankton that had ingested phytoplankton, and, in a second phase, distinguishing different types of phytoplankton. Images from cultures of *Phaeodactylum tricornutum*, a diatom, *Alexandrium minutum*, a dinoflagellate, and *Chlamydomonas reinhardtii*, a freshwater algae, were also included in the datasets for the second phase, in order to increase the efficiency and performance of the second trained Network. Experiments showed excellent testing performances in the discrimination of different types of plankton, evaluated using classical metrics, such as Accuracy, Recall, Precision, F1 score and Mean Average Precision (mAP).

2 MATERIALS AND PROCEDURE

2.1 Study Site and Sample Collection

Sampling was conducted at Cala Santanyí, a beach on the southeastern side of Mallorca (Spain) between June 2021 and mid-September 2022, with two additional dates on 27 September 2022 and 26 October 2022. This beach frequently experiences HABs in summer. The submarine groundwater discharge provides increased nutrient availability for phytoplankton growth (Basterretxea et al., 2010). Additionally, as the beach is very well protected, water renewal is very weak, with shoreward currents generated by the sea breezes pushing water and plankton towards the shore. From June to October 2021 and again from April until mid-September 2022, sampling occurred every 5-10 days, except during phytoplankton blooms, when sampling occurred every 2-3 days. From November 2021 to March 2022, sampling occurred every 10-20 days.

Water samples were collected at approximately the same location. We collected 6 L of water from the surface and 6 L of water from a depth of $\sim$ 1.4 m. After returning to the laboratory, the collected water was passed through a 100 μm filter to remove larger plankton and debris.

2.2 Microplankton Community Sampling and Incubations

Fresh samples were generally processed within 24 hours of collection. Up to 1 L of water from the surface and depth were concentrated to 50 mL using $\leq$ 5 μm filters to retain the microplankton size community of interest. Sub-samples were then processed using a FlowCAM VS series (Yokogawa Fluid Imaging Technologies, Inc) (Yokogawa, 2023). The FlowCAM combines flow cytometry with image microscopy, creating a laminar flow and drawing samples through a flow cell. The camera microscope views the sample through the flow cell and captures an image of any particle it sees using background subtraction. We used the 20x objective setting, meaning objects between 2 μm and 100 μm could be imaged; we ran each sample through the FlowCAM at a rate of 0.05 mL/min for 20 minutes.

From August 2021 to October 2022, 1 L of water from both the surface and depth was incubated for 4–7 days on a 14:10 light:dark cycle. Samples were then condensed and processed in the FlowCAM using the same methodology as with the fresh samples described above.

2.3 Separation of Images

The FlowCAM saves image collages of the objects it photographs. Therefore, it is necessary to crop and separate the images from the collages to obtain and save photographs of individual plankton. All images used in this study were obtained from FlowCAM collages of the fresh or incubated natural samples from Cala Santanyí, and from laboratory monocultures of *P. tricornutum*, *A. minutum*, or *C. reinhardtii*. FlowCAM images of laboratory cultures were obtained on the same FlowCAM VS series using the 20x objective from previous experiments.

2.4 Convolutional Neural Networks (CNNs)

A Convolutional Neural Network is a network used for Deep Learning composed of a set of interconnected layers that consist of several neurons (matrices) which perform successive convolution operations guided by weights and biases (Alzubaidi et al., 2021). Each layer processes grid-like topological data to output also a matrix-type data structure. Weights and biases of neurons are learned and continuously updated as new images get into the training process. CNN models are optimized to minimize the so-called loss function, which is the difference between each prediction output by the CNN model and the corresponding ground-truth. In addition to convolutions, CNN layers can include other operations, such as Linear Unit Rectifications (ReLUs) or Poolings. ReLUs map negative values to 0 and maintain positive values, while Poolings downsample the data packages transmitted to the following layer (Alzubaidi et al., 2021). A CNN can be trained from scratch, but it needs significant computational resources and a huge number of training images. An alternative consists of initializing, retraining, and reconfiguring pre-trained models, a technique commonly known as Transfer Learning (Hussain et al., 2019). This method requires less data and fewer computational resources and is the one used to approach our plankton discrimination problem.

2.5 Differentiation Between Phytoplankton, Zooplankton, and Zooplankton Consuming Phytoplankton

A first dataset composed of 2188 color images from natural sampling contained different types of phytoplankton (PHY), zooplankton (ZOO), and zooplankton consuming phytoplankton (ZCP). Each image showed just one individual, so this first stage solved an image classification problem. Figure 1 shows some examples of zooplankton, phytoplankton and zooplankton consuming phytoplankton. Since each image of the dataset must contain a single organism and were obtained cropping the collates formed by the microscopy, their resolution is not homogeneous, varying with the type, size and form of each individual. For instance, resolutions of images of Figure 1-(a) to (d) were, respectively, 138 $\times$ 160, 119 $\times$ 112, 82 $\times$ 248, and 139 $\times$ 190 pixels, and resolutions of images of Figure 1-(e) to (h) were, respectively, 295 $\times$ 388, 189 $\times$ 192, 134 $\times$ 215, and 168 $\times$ 138 pixels.

This dataset was used to re-train, validate and test an EfficientNetv2 B3 (Tan and Le, 2019) pre-trained model obtained from the Tensor Flow Hub (TensorFlow-Org, 2023). Image resolution required a preadjustment to 300 $\times$ 300 pixels. EfficientNet is one of the most powerful Convolutional Neural Network architectures available online, used worldwide to classify images in numerous relevant applications with excellent results (de Zarzà et al., 2022) (Huang and Liao, 2023). Images containing either PHY, ZOO or ZCP were clustered in 3 completely disjointed groups: Training, Validation and Test, each accounting for 40, 10 and 50% of the whole image set, and distributed as shown in Table 1. The Training and Validation groups were used to re-configure and re-train the EfficientNetv2 B3 model, and the Test group was used to evaluate the performance of the resulting retrained structure with a set of images not involved in the training phase. All aforementioned images were manually classified to generate a ground truth needed for both phases, training and testing: manual classifications are needed for the Neural Network to learn the specific weights and biases of the model, and to quantify the trained model performance comparing each predicted clustering with the corresponding ground truth. During the testing phase, the outputs of the trained model were visually identified as True Positive (TP), True Negative (TN), False Positive (FP), and False Negative (FN) to compute the following metrics:

$$Precision = \frac{TP}{(TP+FP)} \quad Recall = \frac{TP}{(TP+FN)}$$

$$F1-score = \frac{(2*precision*recall)}{(precision+recall)}$$

$$Accuracy = \frac{(TP+TN)}{(TP+TN+FP+FN)}.$$

Figure 1: Samples of zooplankton ((a)-(d)), phytoplankton ((e)-(l)) and zooplankton consuming phytoplankton ((m)-(p)), included in the first dataset. (e)-(h) are diatoms, singles ((e) and (f)) and forming chains ((g) and (h)). (i)-(l) are dinoflagellates.

Table 1: Number of images of each microplankton type used to train, validate, and test the EfficientNetv2 B3 network.

	Training	Validation	Test	Total
ZCP	180	44	224	448
ZOO	112	28	139	279
PHY	585	146	730	1461
Total	877	218	1093	2188

2.6 Object Detection: Identifying Multiple Cells in an Image

One of the challenges with identifying and determining phytoplankton abundance is the ability of dinoflagellates and diatoms, two distinct types of phytoplankton, to form chains. This complicates the identification of different species and also makes it difficult to count the total number of individuals using just image classification. Figures 1-(g)-(h) shows some samples of diatom chains from natural samples.

This second stage centers on phytoplankton and approaches an object classification problem rather than an image classification one. Now, the problem is solved using the fourth version of Ultralitics *You Only Look Once* (YOLO) software infrastructure (Bochkovskiy et al., 2020). YOLO is an open source software package that implements deep learning and neural networks, easy, efficient and proven to perform excellently in object detection and image segmentation in multiple environments (Diwan et al., 2023) (Lee and Hwang, 2022).

More than 5000 color images were manually labeled and clustered into 3 classes: Dinoflagellates, Diatoms and *Chlamydomonas*. Dinoflagellates and diatoms from natural sampling and used in the phytoplankton images of the previous dataset were separated. Monoculture images of *P. tricornutum* were added to the images of diatoms from natural samples, and monoculture images of *A. minutum* were added to the images of dinoflagellates from natural samples. As *C. reinhardtii* is a freshwater algae and not found in marine environments, it was kept in its own class. Labeled images were also split in 3 different groups: Training, Validation and Testing. The ground truth consists of bounding boxes framing each individual of each class found in each image. These bounding boxes found in the Training and Validation images are the elements used by the network to learn the internal weights and biases, instead of the whole images. The resolution of all these images was fixed to 416×416 pixels.

Table 2 shows the number of images and individuals of different classes visually identified in the image set. The last column shows the average number of individuals per class and per image. Table 3 shows the distribution of the individuals of different classes in the three subsets for training, validation and testing.

Original and hand-labeled Testing images were input in the trained model to assess its performance, using Precision, Recall, Accuracy, and F1-score, as defined in section 2.5. In object detection, the *Intersection over Union* (IoU) is defined as the area of the intersection of two bounding boxes over that of their union. A common strategy to evaluate object detectors, such as YOLO v4 in this case, is to select the bounding boxes predicted by the trained model whose detection score exceed a predefined threshold α. Each bounding box output by the network is associated with the ground truth bounding box of the same image that has a maximum IoU, if that IoU exceeds a certain threshold β. The number of True Positives (TP) are the predicted bounding boxes that have been associated with a ground truth bounding box, the False Positives (FP) are the predicted bounding boxes that have not been associated to any ground truth bounding box, and the False Negatives (FN) are the ground truth bounding boxes not associated to any prediction (Padilla et al., 2020). The Precision-Recall Curve is built by computing these metrics for different β values. Then, the pairs of obtained Precisions and Recalls are sorted by the Recall value and plotted. The area below this Precision-Recall Curve will range from 0 to 1, and it is called the Average Precision (AP). A perfect object detector generates AP close to 1, and random object detectors result in a AP around 0.5. The mAP can be defined as the average of AP, for the different classes. A common approach is to use $\beta = 0.5$ (AP@0.5) as a good indicator of detection ability. According to several approaches widely used in Deep Learning, AP and mAP correspond to the same calculation (Wood and Chollet, 2022).

Trainings and Validations were performed under a Google Colaboratory (Google, 2023) environment using a GPU. Colaboratory is a hosted Jupyter Notebook service with no setup required, and ready to use. It provides free access to Machine and Deep learning computing resources, including GPUs and TPUs.

3 EXPERIMENTAL RESULTS

This section gives the first results obtained in two fronts: 1) the assessment of the image classification network used to distinguish among different types of plankton (PHY, ZOO and ZCP), and 2) the evaluation of the object detector model to discriminate among different types of phytoplankton.

Table 2: Number of individuals identified in all the images used to train the object detection network.

Class	Number of Images	Total Number of Individuals	Individuals per image
Chlamydomonas	1520	1666	1.10
Dinoflagellates	2940	3148	1.07
Diatoms	785	2302	2.93
Total	5245	7116	1.35

Table 3: Number of individuals of each class used to train, validate, and test the YOLO network.

Class	Train	Validation	Test
Chlamydomonas	595	458	467
Dinoflagellates	1179	880	881
Diatoms	324	235	226
Total	2098	1573	1574

Table 4: Evaluation metrics for image classification.

Class	Accuracy	Precision	Recall	F1-Score
PHY	97.43%	99.29%	96.84%	98.05%
ZCP	96.43%	87.14%	96.87%	91.75%
ZOO	98.07%	94.73%	90.00%	92.30%

3.1 Image Classification

Table 4 shows the scores of the different metrics used to assess the performance of the image classifier model. Accuracy, Precision and Recall surpass all the 90%, except the Precision in the detection of ZCP, which is greater than 87%. Accordingly, F1-Scores are all $> 90\%$. All these results were obtained from the Testing dataset.

3.2 Object Detection

Table 5 shows the value of the Average Precision with the IoU threshold β fixed in 0.5 (AP@0.5) for the three different types of phytoplankton. The Mean Average Precision computed as the mean of all the AP values included in table 5 is mAP(0.5)= 97.47%, a reference value that indicates a high performance of the trained object classifier.

Figure 2 shows several samples of inferences output by the trained model.

Four diatoms at the top, in the middle, four dinoflagellates and at the bottom, four images with *C. reinhardtii*. Notice how, in the images of diatoms that form chains, each element of the chain is marked separately as one inference of one diatom, although all diatoms inferred in the image form a larger biological structure.

Table 5: Average Precision per class with a β=0.5.

Class	Dinoflagelates	Diatoms	*Chlamy.*
AP(0.5)	99.70%	99.60%	93.10%

4 CONCLUSIONS

This paper advances automatic classification of different species of plankton viewed in images recorded using a FlowCAM. Our approach is based on training CNNs using an extensive and widely assorted image set obtained from field samples collected at a local beach in Mallorca and supplemented with images from monocultures to identify zooplankton and phytoplankton, and to identify different individuals of phytoplankton in a single image. The system, once trained, is a potential solution to separate and taxonomically identify plankton in the thousands of images which can be potentially recorded from microscopic imaging methods, avoiding tedious, slow, and sometimes imprecise manual identification and labeling.

The work has been divided in two parts: firstly, an image classification network trained with a structure based on EfficientNetv2 B3, focused on distinguishing images that contain either phytoplankton or zooplankton; and secondly, a YOLO v4 object classification model trained to discriminate different types of phytoplankton. In the first case, more than 2000 images were used to train the system, and in the second case, more than 7000 individuals of different species from more than 5000 images were input in the YOLO v4 network to be trained, validated and tested. All images involved in both parts were carefully hand-labeled to build the ground truth. The preliminary results show how well the classification succeeds with both models, reaching, in the first one, 90% in terms of F1-Score, and $> 93\%$ of Average Precision with a IoU of 0.5 in the second one.

These results encourage the authors of this paper to extend the work in several directions. Ongoing work is centered on the analysis of results with a wider range of IoU thresholds. However, there are other points that deserve our attention and could also be included in the forthcoming work. Metrics of Precision, Recall, Fall-out and Accuracy need to be analyzed for the different classes of phytoplankton, so that further and more solid conclusions about the classifier performance can be inferred, and see if the model needs to be re-trained with more or different images. Additionally, the image database

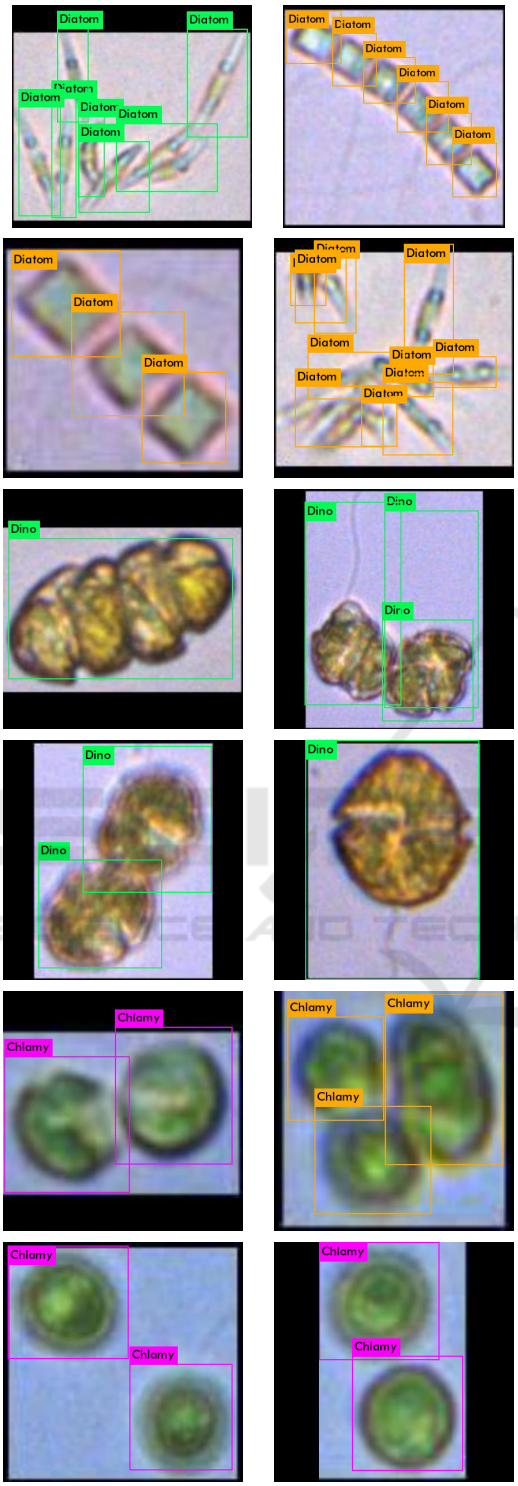

Figure 2: Sample inferences output by the YOLO model.

used to build the different train, validation and testing datasets can be expanded with other samples collected in different areas of the Balearic shoreline and globally to increase and expand the detection of other individuals of other types of plankton organisms. Furthermore, more advanced network infrastructures can be tested, such as the 3 different versions of YOLO v8, the *small*, the *medium* and the *large*; usually, the greater is the size of the trained model, the finest is its performance; however, larger models entail more processing power. Testing different sizes of trained classifiers will permit us to find the compromise between desired or needed detection quality and the available computational resources. All in all, this work has demonstrated the power of the Deep Learning infrastructures to ease and automate the analysis and processing of thousands of images which are obtained from Imaging Microscopy machines like the FlowCAM, and the absolute feasibility for this type of biological applications of CNNs.

ACKNOWLEDGEMENTS

The authors thank Raquel Gutiérez Cuenca, Paula Isabel Gonzalo Valmala, Alba Gómez Rubio, Benjamín Casas, and both current and past members of the InFiBio group for their support collecting and processing water samples from Cala Santanyí.

REFERENCES

Alzubaidi, L., Zhang, J., Humaidi, A., Al-Dujaili, A., Duan, Y., Al-Shamma, O., Santamaría, J., Fadhel, M., Al-Amidie, M., and Farhan., L. (2021). Review of Deep Learning: Concepts, CNN Architectures, Challenges, Applications, Future directions. *Journal of Big Data*, 8(53):12853–12884.

Basterretxea, G., Garcé, E., Jordi, A., and Masó, M. (2007). Modulation of Nearshore Harmful Algal Blooms by in situ Grouth Rate and Water Renewal. *Marine Ecology Progress Series*, 352:53–65.

Basterretxea, G., Tovar-Sánchez, A., Beck, A. J., Masqué, P., Bokuniewicz, H. J., Coffey, R., Duarte, C. M., Garcia-Orellana, J., Garcia-Solsona, E., Martinez-Ribes, L., and Vaquer-Sunyer, R. (2010). Submarine Groudwater Discharge to the Coastal Environment of a Mediterranean Island. *Ecosystem and Biogeochemical Significance. Ecosystems*, 13:629–643.

Bochkovskiy, A., Wang, C.-Y., and Liao, H.-Y. M. (2020). Yolov4: Optimal Speed and Accuracy of Object Detection. https://github.com/ultralytics/, https://arxiv.org/abs/2004.10934.

Buskey, E. J. and Hyatt, C. J. (2006). Use of the FlowCAM for Semi-automated Recognition and Enumeration of

Red Tide Cells (Karenia brevis) in Natural Plankton Simples. *Harmful Algae*, 5(6):685–692.

de Zarzà, I., de Curtò, J., and Calafate, C. T. (2022). Detection of Glaucoma using Three-stage Training with EfficientNet. *Intelligent Systems with Applications*, 16:200140.

Diwan, T., Anirudh, G., and Tembhurne, J. V. (2023). Object Detection using YOLO: Challenges, Architectural Successors, Datasets and Applications. *Multimedia Tools and Applications*, 82(6):9243–9275.

Dubelaar, G. B. and Jonker, R. R. (2000). Flow Cytometry as a Tool for the Study of Phytoplankton. *Scientia Marina*, 64(2):135–156.

Figueroa, R., Garcés, E., Massana, R., and Camp, J. (2008). Description, Host-specificity and Strain Selectivity of the Dinoflagellate Parasite Parvilucifera sinerae sp. Nov. (Perkinsozoa). *Protist*, 159(4):563–578.

Fuchs, R., Thyssen, M., Creach, V., Dugenne, M., Izard, L., Latimier, M., Louchart, A., Marrec, P., Rijkeboer, M., Grégori, G., et al. (2022). Automatic Recognition of Flow Cytometric Phytoplankton Functional Groups using Convolutional Neural Networks. *Limnology and Oceanography: Methods*, 20(7):387–399.

Google (2023). Google Colaboratory: a Hosted Jupyter Notebook Service. https://colab.google/.

Henrichs, D., Anglès, S., Gaonkar, C., and Campbell, L. (2021). Application of a Convolutional Neural Network to Improve Automated Early Warning of Harmful Algal Blooms. *Environmental Science and Pollution Research*, 28:28544–28555.

Huang, M.-L. and Liao, Y.-C. (2023). Stacking Ensemble and ECA-EfficientNetV2 Convolutional Neural Networks on Classification of Multiple Chest Diseases Including COVID-19. *Academic Radiology*, 30(9):1915–1935.

Hussain, M., Bird, J. J., and Faria, D. R. (2019). A Study on CNN Transfer Learning for Image Classification. In *Advances in Computational Intelligence Systems*, pages 191–202.

Kerr, T., Clark, J. R., Fileman, E. S., Widdicombe, C. E., and Pugeault, N. (2020). Collaborative Deep Learning Models to Handle Class Imbalance in FlowCam Plankton Imagery. *IEEE Access*, 8:170013–170032.

Lee, J. and Hwang, K.-i. (2022). YOLO with Adaptive Frame Control for Real-time Object Detection Applications. *Multimedia Tools and Applications*, 81(25):36375–36396.

Menden-Deuer, S., Morison, F., Montalbano, A. L., Franzè, G., Strock, J., Rubin, E., McNair, H., Mouw, C., and Marrec, P. (2020). Multi-Instrument Assessment of Phytoplankton Abundance and Cell Sizes in Mono-Specific Laboratory Cultures and Whole Plankton Community Composition in the North Atlantic. *Frontiers in Marine Sciences*, 7(254).

Padilla, R., Netto, S. L., and da Silva, E. A. B. (2020). A Survey on Performance Metrics for Object-Detection Algorithms. In *Proceedings of the International Conference on Systems, Signals and Image Processing (IWSSIP)*, pages 237–242.

Rodellas, V., Garcia-Orellana, J., Masqué, P., and Weinstein, Y. (2015). Submarine Groundwater Discharge as a Major Source of Nutrients to the Mediterranean Sea. *The Proceedings of the National Academy of Sciencese PNAS*, 112(13):3926–3930.

Sosa-Trejo, D., Bandera, A., González, M., and Hernández-León, S. (2023). Vision-based Techniques for Automatic Marine Plankton Classification. *Artificial Intelligence Reviews*, 56:12853–12884.

Tan, M. and Le, Q. (2019). EfficientNet: Rethinking Model Scaling for Convolutional Neural Networks. In *Proceedings of the 36th International Conference on Machine Learning*, pages 6105–6114.

Tensor-Flow-Org (2023). Tensor Flow Hub, a Repository of Trained Machine Learning Models. https://www.tensorflow.org/hub.

Tovar-Sánchez, A., Basterretxea, G., Rodellas, V., Sánchez-Quiles, D., García-Orellana, J., Masqué, P., Jordi, A., López, J. M., and Garcia-Solsona, E. (2014). Contribution of Groundwater Discharge to the Coastal Dissolved Nutrients and Trace Metal Concentrations in Majorca Island: Karstic vs. Detrital Systems. *Environ Sci. Technol*, 48:11819–11827.

Ullah, I., Carrión-Ojeda, D., Escalera, S., Guyon, I. M., Huisman, M., Mohr, F., van Rijn, J. N., Sun, H., Vanschoren, J., and Vu, P. A. (2022). Meta-Album: Multi-domain Meta-Dataset for Few-Shot Image Classification. In *Neural Information Processing Systems*.

Wood, L. and Chollet, F. (2022). Efficient Graph-Friendly COCO Metric Computation for Train-Time Model Evaluation. https://arxiv.org/abs/2207.12120.

Yamazaki, H. (2022). Plankton Image Dataset from a Cabled Observatory System (JEDI System/OCEANS) Deployed at Coastal Area of Oshima Island, Tokyo, Japan. https://doi.org/10.48518/00014.

Yokogawa (2023). FlowCam: Flow Imaging Microscopy. https://www.yokogawa.com/solutions/products-and-services/life-science/flowcam-flow-imaging-microscopy/.

Zhang, J., Li, C., Yin, Y., Zhang, J., and Grzegorzek, M. (2023). Applications of Artificial Neural Networks in Microorganism Image Analisis: a Comprehensive Review from Conventional Multilayer Perceptron to Popular Convolutional Neural Network and Potential Visual Transformer. *Artificial Intelligence Review*, 56:1013–1070.

Zhang, Y., Lu, Y., Wang, H., Chen, P., and Liang, R. (2021). Automatic Classification of Marine Plankton with Digital Holography Using Convolutional Neural Network. *Optics and Laser Technology*, 139:106979.

Zingone, A., Escalera, L., Aligizaki, K., Fernández-Tejedor, M., Ismael, A., Montresor, M., Mozetič, P., Taş, S., and Totti, C. (2021). Toxic Marine Microalgae and Noxious Blooms in the Mediterranean Sea: A Contribution to the Global HAB Status Report. *Harmful Algae*, 102:101843.